A HUBBLE SPACE TELESCOPE CENSUS OF NUCLEAR STAR CLUSTERS IN LATE-TYPE SPIRAL GALAXIES. II. CLUSTER SIZES AND STRUCTURAL PARAMETER CORRELATIONS

Torsten Böker,[1] Marc Sarzi,[2] Dean E. McLaughlin,[3] Roeland P. van der Marel,[3]
Hans-Walter Rix,[4] Luis C. Ho,[5] and Joseph C. Shields[6]

ABSTRACT

We investigate the structural properties of nuclear star clusters in late-type spiral galaxies. More specifically, we fit analytical models to Hubble Space Telescope images of 39 nuclear clusters in order to determine their effective radii after correction for the instrumental point-spread function. We use the results of this analysis to compare the luminosities and sizes of nuclear star clusters to those of other ellipsoidal stellar systems, in particular the Milky Way globular clusters. Our nuclear clusters have a median effective radius of $\bar{r}_e = 3.5$ pc, with 50% of the sample falling in the range 2.4 pc $\leq r_e \leq$ 5.0 pc. This narrow size distribution is statistically indistinguishable from that of Galactic globular clusters, even though the nuclear clusters are, on average, 4 mag brighter than the old globular clusters. We discuss some possible interpretations of this result. From a comparison of nuclear cluster luminosities with various properties of their host galaxies, we confirm that more luminous galaxies harbor more luminous nuclear clusters. It remains unclear whether this correlation mainly reflects the influence of galaxy size, mass, and/or star formation rate. Since the brighter galaxies in our sample typically have stellar disks with a higher central surface brightness, nuclear cluster luminosity also correlates with this property of their hosts. On the other hand, we find no evidence for a correlation between the presence of a nuclear star cluster and the presence of a large-scale stellar bar.

Key words: galaxies: nuclei — galaxies: spiral — galaxies: star clusters

1. INTRODUCTION

In most formation scenarios for spiral galaxies, the central bulge is the "trash bin of violent relaxation," where a dynamically hot stellar component has formed either through external potential perturbations, such as early mergers of protogalaxies (see, e.g., Carlberg 1992), or perhaps via internal effects, such as violent bar instabilities (Norman, Sellwood, & Hasan 1996). While this "nature or nurture" debate is far from settled, the recent discovery of the so-called M-σ relation (Gebhardt et al. 2000; Ferrarese & Merritt 2000) has made it clear that the structure of the very nucleus, i.e., the black hole and its immediate vicinity ($\ll 1$ pc), is closely linked to the overall dynamical structure of the stellar bulge. The latest-type spiral galaxies, then, must have lived very sheltered and uneventful lives, since their central trash bin is virtually empty. Indeed, these disk-dominated, bulgeless galaxies (see, e.g., Matthews & Gallagher 1997) often have slowly rising rotation curves, which indicate a nearly homogeneous mass distribution on scales $\lesssim 1$ kpc. On these scales, gravity therefore hardly provides a vector pointing at the center, and it is not obvious that the nucleus of these galaxies is well defined and is a unique environment.

It therefore came as a surprise that recent observations with the Hubble Space Telescope (HST) have shown that the photocenter of many late-type spiral galaxies is occupied by a compact, luminous stellar cluster (Phillips et al. 1996; Carollo, Stiavelli, & Mack 1998; Matthews et al. 1999). In a recent paper (Böker et al. 2002, hereafter Paper I), we have shown that at least 75% of spiral galaxies with Hubble types later than Sc harbor such a nuclear star cluster. The fraction of nuclear clusters (NCs) appears to be somewhat lower in earlier Hubble types, as indicated by the results of Carollo et al. (1998). However, smaller sample sizes and the observational difficulties arising from the more complex nuclear morphologies of early-type spiral galaxies and the decreasing contrast between a central star cluster and a luminous bulge make this result somewhat uncertain. Typical luminosities of NCs are in the range 10^6–10^7 $L_\odot$ (Paper I), which makes them much brighter than average stellar clusters in the disks of nearby spiral galaxies (Larsen 2002) and comparable to young "super star clusters" in luminous merger pairs (see, e.g., Whitmore et al. 1999) or circumnuclear star-forming rings in spiral galaxies (see, e.g., Maoz et al. 2001).

Despite the recent progress, the formation mechanism of NCs remains largely a mystery. So far, no satisfying explanation has been put forward for the high gas densities that must have been present to enable the in situ formation of such compact and luminous objects in the nuclei of these disk galaxies with shallow potentials. Plausible alternatives to in situ formation include the infall of evolved clusters, possibly combined with more recent star formation events due to the accretion of gas in the galaxy nucleus. In order to gather evidence for or against any of these scenarios, it is essential to identify the stellar population(s) that comprise the NC, and thus to constrain the cluster formation history. Another

[1] Astrophysics Division, RSSD, European Space Agency, ESTEC, NL-2200 AG Noordwijk, Netherlands.
[2] University of Oxford, Keble Road, Oxford OX1 3RH, England.
[3] Space Telescope Science Institute, 3700 San Martin Drive, Baltimore, MD 21218.
[4] Max-Planck-Institut für Astronomie, Königsstuhl 17, D-69117 Heidelberg, Germany.
[5] Observatories of the Carnegie Institution of Washington, 813 Santa Barbara Street, Pasadena, CA 91101-1292.
[6] Department of Physics and Astronomy, Clippinger Research Laboratories, Ohio University, 251B, Athens, OH 45701-2979.

crucial piece of information in this undertaking is an accurate estimate for the cluster mass.

The stellar masses of NCs can be derived, under the assumption of spherical symmetry, if one has accurate knowledge of (1) the stellar velocity dispersion and (2) the cluster light distribution. This kind of analysis has been successfully applied to NCs (Böker, van der Marel, & Vacca 1999), as well as young clusters in the disks of nearby galaxies (Smith & Gallagher 2001; Mengel et al. 2002). Our team has obtained high-resolution spectroscopy of ≈ 15 clusters from the sample of Paper I. These data will address point 1 above, i.e., to accurately measure the stellar velocity dispersion of the clusters (Walcher et al. 2003,[7] 2004). The purpose of the present paper is to discuss point 2, namely, the size and spatial structure of the NC sample of Paper I. Because these objects are only barely resolved even with *HST*, one has to carefully correct for the effects of the instrumental point-spread function (PSF). Because standard deconvolution algorithms are not well suited to the realm of "almost point sources," we have used the specialized software package ISHAPE (Larsen 1999) to find the best match between the data and PSF-convolved analytical models for the cluster shapes. We describe the details of this exercise in § 2 and compare the resulting structural parameters of NCs to those of other cluster populations in § 3.

Because nuclear star clusters are a relatively new aspect of galaxy morphology, it seems a logical approach to search for correlations between the properties of NCs and those of their host galaxies. As has been shown by Carollo (1999) for spiral galaxies of earlier Hubble type, such empirical correlations might reveal clues about the mechanism(s) that regulate the gas supply in the very centers of spiral galaxies and will certainly improve our understanding of nuclear activity in spiral galaxies. Moreover, because the presence of an NC appears to be a common feature in all types of spiral galaxies, the dynamical processes that lead to nuclear starbursts will be an important contribution to the discussion of bulge formation scenarios and a possible evolutionary connection between the various Hubble types. For these reasons, we present in § 4 a number of correlation plots between NC sizes/luminosities and various host galaxy properties, such as size, Hubble type, H I mass, star formation rate (SFR), or total magnitude. We summarize our results in § 5.

2. STRUCTURAL ANALYSIS OF NUCLEAR STAR CLUSTERS

2.1. *Methodology*

Star clusters in all but the closest galaxies are marginally resolved sources, even with the excellent resolution of *HST* images. In order to measure reliably their intrinsic sizes and structural parameters, it is therefore crucial to have both observations with high signal-to-noise ratio (S/N) *and* accurate knowledge of the instrumental PSF. Insufficient sampling of the PSF can complicate matters further. For example, the pixel size of the WFPC2 (0″1 and 0″0455 for the WF and PC chips, respectively) in general does not provide Nyquist sampling of the *HST* resolution element $R = \lambda/D$. While subpixel dithering can alleviate this problem to some extent, *HST* observations of extragalactic star clusters in all but the closest galaxies are almost always confined to the regime of "marginally resolved."

In this situation, none of the conventional deconvolution methods, such as the maximum entropy principle (Burch, Gull, & Skilling 1983) or the Richardson-Lucy algorithm (Richardson 1972; Lucy 1974), work reliably. Instead, differential aperture photometry (e.g., the magnitude difference $m_2 - m_4$ between concentric apertures of 2 and 4 pixels; Holtzman et al. 1992) of stellar clusters and comparison to individual stars broadened by Gaussians has been used to estimate cluster sizes. However, a Gaussian is generally a poor approximation to the surface brightness profile of stellar clusters. In particular, the wings of a Gaussian fall off too rapidly and cannot adequately describe the outer regions of either old globular clusters (GCs) in the Milky Way or young GCs in external galaxies.

More recently, a number of authors (e.g., Kundu & Whitmore 1998; Larsen 1999; Carlson & Holtzman 2001) have independently developed techniques to determine more reliably the structure of stellar clusters in external galaxies. The various methods are conceptually similar in that they assume a parametric model for the intrinsic light distribution. A particular model is considered to be a good description of reality if, after convolution with the instrumental PSF, it matches the observations. The "best" model is the one that minimizes the χ^2 difference to the data. The most widely used analytic models for the projected density profile of stellar clusters are those of King (1962):

$$f(z) = \begin{cases} \left(\dfrac{1}{\sqrt{1+z^2}} - \dfrac{1}{\sqrt{1+c^2}} \right)^2, & \text{for } z < c, \\ 0, & \text{for } z \geq c. \end{cases} \quad (1)$$

Here z is defined by $z^2 = a_1 x^2 + a_2 y^2 + a_3 xy$, with x and y denoting the coordinates relative to the center of the profile and with the constants a_1, a_2, and a_3, which depend on the major axis, ellipticity, and orientation of the model. The so-called concentration index c is the ratio between the tidal radius r_t and the core radius r_c.

In the regime of marginal resolution, the results of Carlson & Holtzman (2001) have shown that unless the S/N of the observations is exceptionally high ($\gtrsim 500$), it is very difficult to distinguish between King models of different concentration indices. On the other hand, they find that the effective radius r_e, i.e., the radius that contains half the cluster light in projection, can be fairly robustly estimated. The value of r_e does not depend strongly on the exact shape of the assumed model. This is in agreement with the results of Kundu & Whitmore (1998) and has been extensively tested by Larsen (1999). In what follows, we will describe our attempts to measure the effective radii of the NCs found in the survey of Paper I.

For our analysis, we have made use of Sören Larsen's software package ISHAPE, which is described in detail in Larsen (1999). This software package has been well tested in a number of studies (e.g., Mengel et al. 2002; Larsen et al. 2002b) and has proved to be a robust and user-friendly tool for structural studies of compact star clusters. In brief, the program convolves a two-dimensional analytical model (e.g., Gauss, Hubble, Moffat, or King profiles) with a user-provided PSF and finds the particular parameter set that best describes the observations, including the exact location of the cluster centroid on subpixel scales. Comparison with the pure PSF (i.e., a PSF-convolved δ-function) allows one to assess

---

[7] Walcher et al. (2003) is available at http://www.ociw.edu/ociw/symposia/series/symposium1/proceedings.html.

whether the clusters are resolved at *HST* resolution. Because r_e is not defined for functions with divergent integrals such as Hubble-type profiles, we have only attempted to fit the data with the above-mentioned King models, as well as Moffat profiles, which are defined as

$$f(z) = \frac{1}{(1 + z^2)^i}, \qquad (2)$$

with z defined as for the King model and $i > 1$ denoting the so-called power index.

In order to construct accurate PSFs for our analysis, we have used the TinyTim software (Krist & Hook 2001), which accounts for the spectral passband used, the plate scale variations across the field of view, and the spectral energy distribution (SED) of the source. Although all of our images were taken through the same filter (F814W), we have constructed a separate PSF, according to the exact position of the NC on the detector array. We note, however, that this only marginally affects the results because the WFPC2 PSF varies only slightly across the PC field. The choice of the correct SED for constructing the PSF is somewhat more critical in estimating the NC sizes. Unfortunately, spectroscopic information is available for only a limited number of NCs. Early results of our spectroscopic follow-up survey (Walcher et al. 2003) show that the light of many NCs is dominated by a stellar population in the age range 50–300 Myr. This agrees with a number of case studies of individual clusters, e.g., in M33 (Gordon et al. 1999), NGC 2403 (Davidge & Courteau 2002), IC 342 (Böker et al. 1999), or NGC 4449 (Böker et al. 2001). We therefore chose the SED of an A5 star for constructing the TinyTim PSF for all objects. We have verified that an alternate choice for the cluster SED, e.g., that of a cool giant with spectral type M3, does not significantly change the ISHAPE results.

2.2. *Results*

We have used ISHAPE to fit all 59 NCs of Paper I within the aperture radius that is dominated by emission from the NC (at least $5r_e$). Some typical examples that illustrate the ISHAPE results are presented in Figure 1. We used only circularly symmetric models within ISHAPE because visual inspection of the fit results confirmed that the majority of clusters show little evidence for flattening. In a few cases, the clusters are asymmetric or have a complex morphology, most likely due to dust lanes or faint companion clusters. These objects were excluded from the ISHAPE analysis. In addition, we excluded those clusters with insufficient S/N to obtain reliable fits, i.e., with S/N < 40 (Larsen 1999).

The remaining 39 clusters were fitted using King profiles with $c \equiv r_t/r_c$ values of 15, 30, and 100, as well as Moffat profiles with power indices of $i = 1.5$ and 2.5. In principle, the galaxy light underlying the NC must be subtracted before fitting the cluster profile. The ISHAPE code simply subtracts a constant background level, measured at the edge of the fitting aperture. While this algorithm is certainly less than perfect, and more sophisticated methods to fit the surface brightness profile of the galaxy disk could be employed, we have verified that the resulting values for r_e are not systematically biased by this shortcoming. In fact, the cluster magnitudes calculated by integrating the best-fit ISHAPE model agree well with those listed in Paper I, which were derived with a more careful estimation of the galaxy background (see § 3.1). The median (mean) difference between these two sets of numbers is 0.07 (0.11) mag

when integrating the models over the same aperture used for the Paper I photometry.

The best-fitting models and the resulting effective radii, in both angular and physical dimensions, are summarized in Table 1. The majority (29/39) of NCs have $r_e < 5$ pc, with median (mean) values of 3.5 (5.1) pc. As discussed further in § 3, these values are comparable to the typical size of old GCs in the Milky Way and other nearby galaxies. We emphasize that all clusters are resolved; i.e., models that simply rescale and position the TinyTim PSFs are inconsistent with the data by a large margin. For completeness, we also list in Table 1 the best-fitting analytic model. We caution, however, that in some cases, other models may also be consistent with the data. However, this has little impact on the uncertainties of the r_e measurements, as explained further below. Our goal is not to determine the detailed shape of the cluster profile, but merely to obtain a robust estimate for its size.

The uncertainties listed in column (7) of Table 1 represent the range of r_e values for the best-fitting model profile that yields acceptable fits to the data. Here, "acceptable" is defined by the 3 σ confidence limit for one free parameter, i.e., $\Delta\chi^2 < 9$ (see, e.g., Press et al. 1992). Our analysis is conservative in the following sense: before evaluating the quality of the model fits, we rescaled all χ^2 values such that the best ISHAPE model for a given galaxy had a χ^2 value equal to the number of degrees of freedom, i.e., the number of data points (pixels in the aperture) minus the number of free parameters. This rescaling was necessary because ISHAPE appears to underestimate the intrinsic errors in the cluster images. As a result, many of the best χ^2 values do not formally represent "good" models according to χ^2 statistics. Since the scale factor was always smaller than 1, the χ^2 rescaling is equivalent to increasing the noise level of each data point or pixel, and it consequently broadens the range of models that appear consistent with the data. Unfortunately, this rescaling of errors made a more rigorous statistical comparison between the different analytic profiles impossible.

To illustrate the analysis, Figure 2 shows, for the example of NGC 2805, the rescaled χ^2 values as a function of r_e for all models considered. In this case, a Moffat profile with a power index of 1.5 (MOFFAT15) and effective radius $r_e = 0\rlap.{''}056 \pm 0\rlap.{''}003$ yields the best fit to the data. The 3 σ confidence limit and the corresponding range of r_e is indicated by the horizontal line in the inset panel. As mentioned before, the effective radius is a rather robust quantity; i.e., different models yield similar values for r_e, even if they are not formally consistent with the data according to the above criterion for $\Delta\chi^2$. In the case of NGC 2805, this can be seen in Figure 2: the "best" values for r_e of all five models are within 20% of each other, which is also the typical uncertainty listed in Table 1.

3. DISCUSSION OF STRUCTURAL PARAMETERS

3.1. *Comparison to Milky Way Globular Clusters*

A natural question to address with the data we have in hand is that of a possible size-luminosity relation for NCs. Since NCs in late-type disks are potential candidates for the seeds of bulge formation, they might follow the mass-radius correlation established for more massive ellipsoidal stellar populations, i.e., elliptical galaxies and bulges of intermediate- and early-type spiral galaxies (see, e.g., Kormendy 1985; Bender, Burstein, & Faber 1992). On the other hand, the old GCs in the Milky Way, which constitute the best-studied family of stellar clusters, are remarkably free of any such trend; the effective radii of Galactic GCs are independent of cluster luminosity or mass
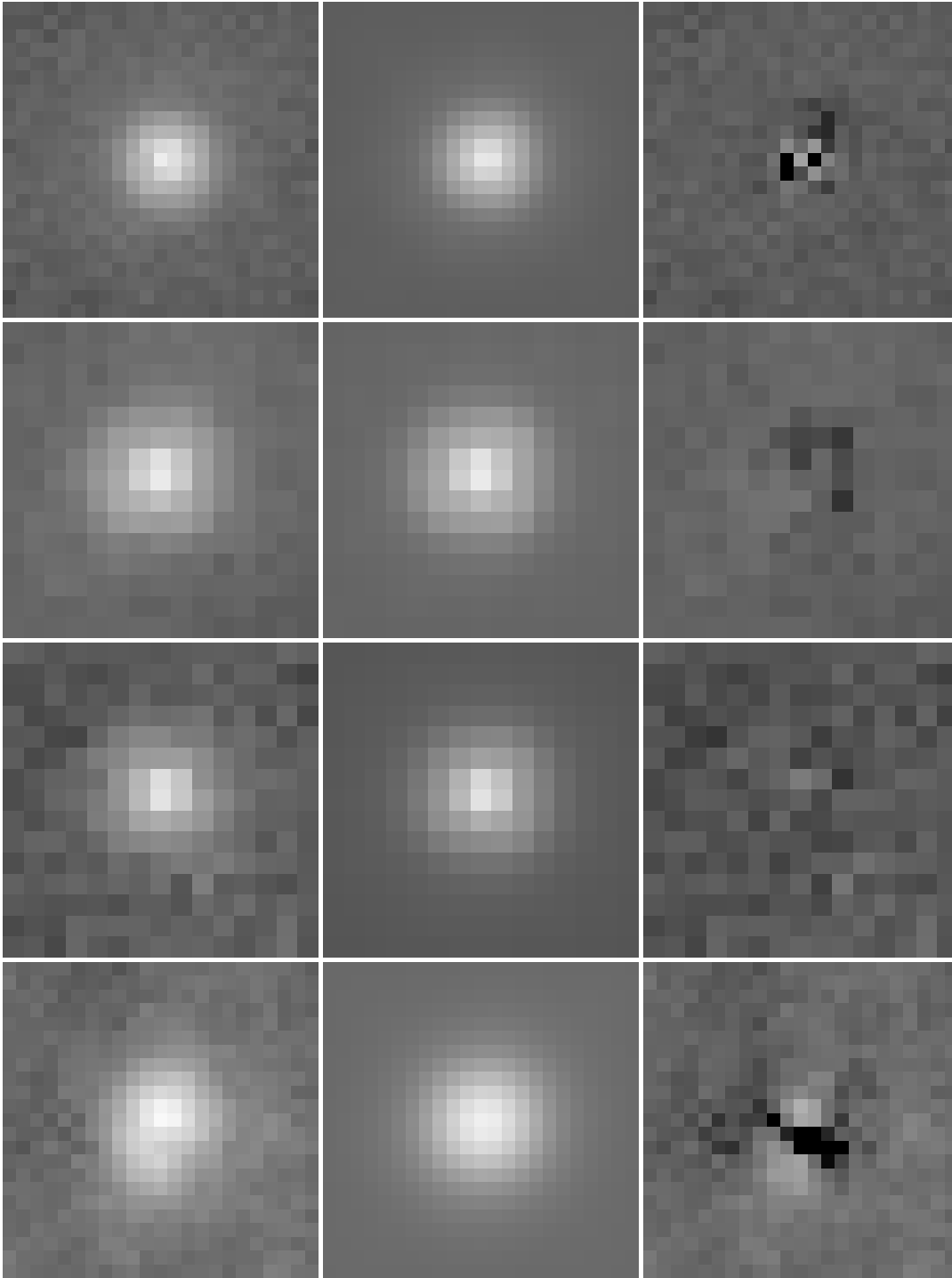
FIG. 1.—Some typical examples of ISHAPE fits. The three panels of each row show (*from left to right*) the data, the best ISHAPE fit (analytic model convolved with TinyTim PSF), and the residuals (data − fit). The field size of each panel corresponds to the aperture radius R_u (Paper I) over which the NC dominates the emission. From top to bottom, the objects are NGC 2805, NGC 3445, NGC 3906, and NGC 4618. The last was excluded from the analysis because of its complex morphology, which prevented a good fit.

(van den Bergh, Morbey, & Pazder 1991; Djorgovski & Meylan 1994; McLaughlin 2000). The same is true for GCs in the nearby galaxies M31 (Barmby, Holland, & Huchra 2002), M33 (Larsen et al. 2002a), and NGC 5128 (Harris et al. 2002).

In Figure 3, we plot the absolute *I*-band magnitude of the NCs, M_I^C, against their effective radius, r_e. The procedure for measuring M_I^C is described in detail in Paper I. In brief, the challenge is to determine the light contribution of the stellar disk underlying the NCs. For this, we use two limiting models

for the inward extrapolation of the galaxy disk profile. The M_I^C values in column (5) of Table 1 represent the average of the resulting two numbers; half of their difference determines the size of the error bars in Figure 3. Aside from a handful of bright clusters with effective radii larger than average, the bulk of the sample—28 of 39 clusters—is found in the narrow range 1 pc $\leq r_e \leq$ 5 pc, while the clusters range over a factor of $\sim$100 in luminosity, $-9 \gtrsim M_I \gtrsim -14$. As we discuss below, relating luminosity to mass is nontrivial for NCs, but taken at

TABLE 1
SUMMARY OF CLUSTER PROPERTIES

Galaxy (1)	Distance (Mpc) (2)	Disk μ_I^0 (mag arcsec^{-2}) (3)	m_I^C (mag) (4)	M_I^C (mag) (5)	Best Model (6)	r_e (arcsec) (7)	r_e (pc) (8)	log I_e ($L_\odot$ pc^{-2}) (9)
A1156+52.........	18.7	19.21	20.43	−10.98	King100	0.025 ± 0.006	2.27	4.52
ESO 138-10	13.5	15.06	16.64	−14.44	King15	0.104 ± 0.041	6.81	4.94
ESO 202-41	19.9	20.58	22.51	−9.01	ngf[a]	. . .	. . .	. . .
ESO 241-6	17.4	18.35	21.24	−9.99	ngf[a]	. . .	. . .	. . .
ESO 290-39	19.1	20.41	22.52	−8.92	ngf[a]	. . .	. . .	. . .
ESO 358-5	20.1	20.62	20.09	−11.45	King100	0.046 ± 0.004	4.48	4.11
ESO 418-8	14.1	19.02	20.54	−10.24	Moffat15	0.019 ± 0.005	1.30	4.70
ESO 504-30	23.9	19.20	20.70	−11.34	King100	0.047 ± 0.012	5.45	3.90
NGC 0275........	24.0	18.30	19.47	−12.54	King100	0.030 ± 0.004	3.49	4.76
NGC 0300........	2.2	18.75	15.29	−11.43	King30	0.272 ± 0.066	2.90	4.48
NGC 0337a........	14.3	19.93	20.62	−10.34	ngf[a]	. . .	. . .	. . .
NGC 0428........	16.1	18.68	17.94	−13.15	King100	0.043 ± 0.002	3.36	5.04
NGC 0450........	25.6	18.00	20.07	−11.96	King100	0.196 ± 0.050	24.33	2.85
NGC 0600........	25.2	18.54	19.91	−12.17	King100	0.024 ± 0.003	2.93	4.77
NGC 0853........	20.2	17.89	19.89	−11.68	King30	0.035 ± 0.004	3.43	4.44
NGC 1042........	18.2	14.69	18.22	−13.14	King100	0.022 ± 0.005	1.94	5.51
NGC 1493........	11.4	17.27	17.17	−13.13	Moffat15	0.047 ± 0.005	2.60	5.26
NGC 2139........	23.6	15.80	19.09	−12.83	ngf[b]	. . .	. . .	. . .
NGC 2552........	9.9	19.69	18.04	−12.04	King100	0.046 ± 0.004	2.21	4.96
NGC 2763........	25.3	16.41	20.33	−11.83	Moffat25	0.019 ± 0.004	2.33	4.83
NGC 2805........	28.1	18.03	19.02	−13.33	Moffat15	0.056 ± 0.003	7.63	4.40
NGC 3346........	18.8	18.12	19.64	−11.78	King100	0.020 ± 0.003	1.82	5.03
NGC 3423........	14.6	17.36	19.03	−11.85	King100	0.059 ± 0.008	4.18	4.33
NGC 3445........	32.1	17.57	19.10	−13.45	King100	0.024 ± 0.005	3.73	5.07
NGC 3782........	13.5	18.20	20.61	−10.07	Moffat15	0.029 ± 0.007	1.90	4.31
NGC 3906........	16.7	18.64	21.12	−10.04	King100	0.047 ± 0.013	3.81	3.69
NGC 3913........	17.0	17.60	21.21	−9.97	ngf[b]	. . .	. . .	. . .
NGC 4027........	22.7	16.73	20.27	−11.59	ngf[b]	. . .	. . .	. . .
NGC 4204........	13.8	19.42	20.51	−10.26	King100	0.052 ± 0.011	3.48	3.85
NGC 4299........	16.8	17.73	19.46	−11.73	King100	0.016 ± 0.004	1.30	5.30
NGC 4411b........	19.1	16.92	18.88	−12.58	King100	0.097 ± 0.007	8.98	3.96
NGC 4416........	20.7	17.91	22.10	−9.53	ngf[a]	. . .	. . .	. . .
NGC 4487........	14.6	17.01	17.89	−12.97	Moffat15	0.010 ± 0.003	0.71	6.32
NGC 4496a......	25.3	18.59	20.08	−11.99	Moffat15	0.020 ± 0.003	2.45	4.85
NGC 4540........	19.8	17.64	19.25	−12.29	ngf[b]	. . .	. . .	. . .
NGC 4618........	10.7	18.02	18.73	−11.46	ngf[b]	. . .	. . .	. . .
NGC 4625........	11.7	16.80	19.74	−10.63	King100	0.508 ± 0.040	28.81	2.17
NGC 4701........	11.0	15.91	16.80	−13.46	King100	0.046 ± 0.001	2.45	5.44
NGC 4775........	22.4	16.82	18.04	−13.78	King100	0.039 ± 0.004	4.24	5.09
NGC 5068........	8.7	18.21	17.54	−12.34	King30	0.177 ± 0.064	7.47	4.03
NGC 5584........	24.2	17.68	21.91	−10.08	ngf[a]	. . .	. . .	. . .
NGC 5585........	8.2	17.92	18.24	−11.35	King100	0.082 ± 0.006	3.26	4.35
NGC 5668........	23.8	17.80	18.85	−13.10	King100	0.038 ± 0.004	4.38	4.79
NGC 5669........	21.2	18.45	21.65	−10.03	ngf[a]	. . .	. . .	. . .
NGC 5774.......	23.5	18.78	21.96	−9.98	ngf[a]	. . .	. . .	. . .
NGC 5964.......	22.2	18.43	19.21	−12.63	King100	0.046 ± 0.003	4.95	4.50
NGC 6509........	27.5	17.39	19.48	−13.09	King100	0.021 ± 0.005	2.80	5.18
NGC 7418........	18.4	14.64	15.02	−16.34	ngf[b]	. . .	. . .	. . .
NGC 7424........	10.9	17.23	18.79	−11.42	ngf[b]	. . .	. . .	. . .
NGC 7689........	24.9	16.49	18.22	−13.78	ngf[b]	. . .	. . .	. . .
NGC 7793........	3.3	17.59	13.99	−13.64	King100	0.484 ± 0.006	7.74	4.51
UGC 3574........	23.4	18.35	19.97	−11.98	King100	0.068 ± 0.008	7.71	3.85
UGC 3826........	27.8	19.11	21.59	−10.76	ngf[a]	. . .	. . .	. . .
UGC 4499........	12.5	19.83	21.91	−8.65	ngf[a]	. . .	. . .	. . .
UGC 4988........	24.2	19.23	20.76	−11.20	King100	0.030 ± 0.006	3.52	4.22
UGC 5015........	25.7	19.14	20.71	−11.37	King30	0.060 ± 0.017	7.48	3.64
UGC 6931........	20.7	20.15	21.87	−9.75	ngf[a]	. . .	. . .	. . .
UGC 8516........	16.5	18.15	20.16	−10.99	ngf[b]	. . .	. . .	. . .
UGC 12732......	12.4	20.14	19.35	−11.29	King100	0.065 ± 0.003	3.91	4.17

NOTES.—Col. (2): Galaxy distance from Paper I. Col. (3): Observed (i.e., not inclination-corrected) peak surface brightness of the galaxy disk (underlying the NC). Col. (4): Apparent I-band magnitude of NC. Col. (5): Absolute I-band magnitude of NC, corrected for foreground reddening. Col. (6): Name of best-fitting ISHAPE model; "ngf" means that no good fit was possible, because of either low S/N data (footnote a) or a complex morphology (footnote b). Col. (7) Angular effective radius and uncertainty as discussed in § 2. Col. (8) Effective radius in parsecs. Col. (9) Logarithm of effective I-band intensity of NC, defined as $\log I_e = 0.4(4.08 − M_I^C) − \log (2\pi r_e^2)$ for r_e in parsecs.

[a] No good fit was possible because of low-S/N data.
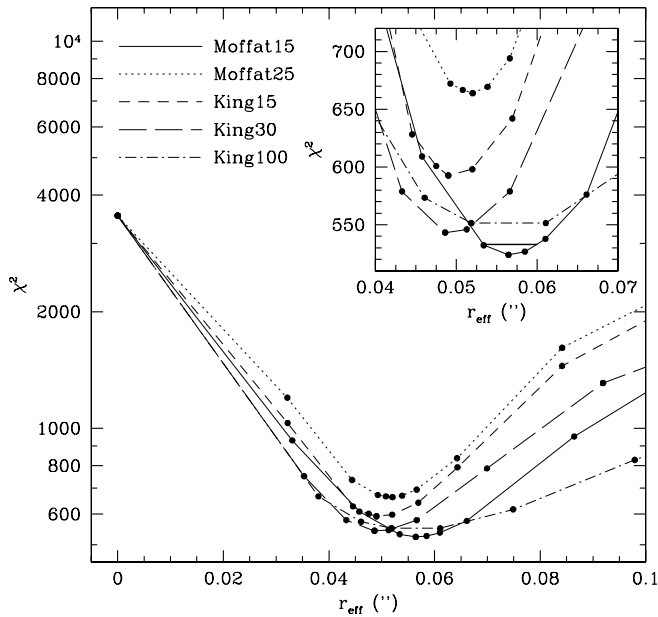[b] No good fit was possible because of a complex morphology.

FIG. 2.—ISHAPE fit results for NGC 2805. Shown are the χ^2 values of each fit as a function of effective radius for all analytic models explored. These values have been rescaled such that the minimum χ^2 matches the number of degrees of freedom (see text). The inset panel shows that only the MOFFAT15 model with r_e values of $0\rlap{.}''056 \pm 0\rlap{.}''006$ falls below the 3 σ confidence limit for five free parameters ($\Delta\chi^2 = 18.2$; *horizontal dashed line*). Within the MOFFAT15 model, the range of acceptable values for r_e is marked by the solid horizontal line, which denotes the 3 σ confidence limit for a single free parameter ($\Delta\chi^2 = 9$).

face value, the situation illustrated in Figure 3 is more reminiscent of GCs than of the bulges in early-type spiral galaxies.

It is not only the absence of a correlation between size and luminosity that appears to connect the NCs in our sample to GCs. As noted in § 2.2, the distribution of r_e for our NC sample is quantitatively similar to that of Galactic GCs. This is shown explicitly in Figure 4, where we also compare the distributions of the I-band magnitude for our NC sample and for 111 Milky Way GCs without an obvious or suspected core-collapse morphology, i.e., with well-determined r_e values.[8] Evidently, although the median M_I of NCs is fully 3–4 mag brighter than that of the Milky Way GCs, the widths of the two luminosity distributions (which correspond to a distribution in mass for the GCs) are comparable. The median effective radius of the NCs is $\bar{r}_e = 3.5$ pc (interquartile range 2.4–5.0 pc), and that of the GCs is $\bar{r}_e = 3.3$ pc (interquartile range 2.4–5.2 pc). A two-sample Kolmogorov-Smirnov (KS) test confirms statistically the visual impression that the two r_e distributions are identical, with a probability $P_{\rm KS} = 0.75$ that they have been drawn from the same parent distribution. We further note that the GCs in M31, M33, and NGC 5128 have essentially the same median r_e as the clusters in Figure 4 and the same independence from cluster luminosity (see the references above).

Figure 5 provides an alternate illustration of this basic point, in a representation that allows for direct comparison with larger ellipsoidal stellar systems and comes closer to the "fundamental plane" typically plotted for such systems. Here we show the average surface brightness, $I_e \equiv L_I/(2\pi r_e^2)$, versus effective radius r_e for the NCs, the 111 Galactic GCs from the Harris (1996) catalog, and a number of E galaxies, spiral bulges, and dwarf elliptical (dE) galaxies from the compilation of Burstein et al. (1997). The position of Milky Way GCs and NCs to the left of the plot shows again that the latter have essentially the same size as the former, but are substantially brighter and therefore at higher surface brightness.

Of additional interest is the disconnect between the GCs and NCs on the one hand and the elliptical galaxies and spiral bulges on the other, a dichotomy first noted by Kormendy (1985). As we mentioned at the beginning of this discussion, the bulges and galaxies show a size-luminosity relation, while GCs do not.

Equivalently, GCs have an enormous spread in surface brightness, while bulges and elliptical galaxies at a given r_e appear much more uniform. Although this fact is still not well understood, the alignment of our NCs with the GCs in Figure 5 would seem to underline a closer link between NCs and GCs, as opposed to one between NCs and classical galaxy bulges.

For completeness, we have included in Figure 5 data for the nuclei of five nucleated dE galaxies in Virgo, from the sample of Geha, Guhathakurta, & van der Marel (2002). As those authors have already demonstrated, with a different version of the fundamental plane, the dwarf elliptical nuclei are also more similar to star clusters than to galaxy bulges.

3.2. *Possible Interpretations*

The apparent similarity between NCs and GCs could be an important clue to the nature and origin of the NCs themselves.
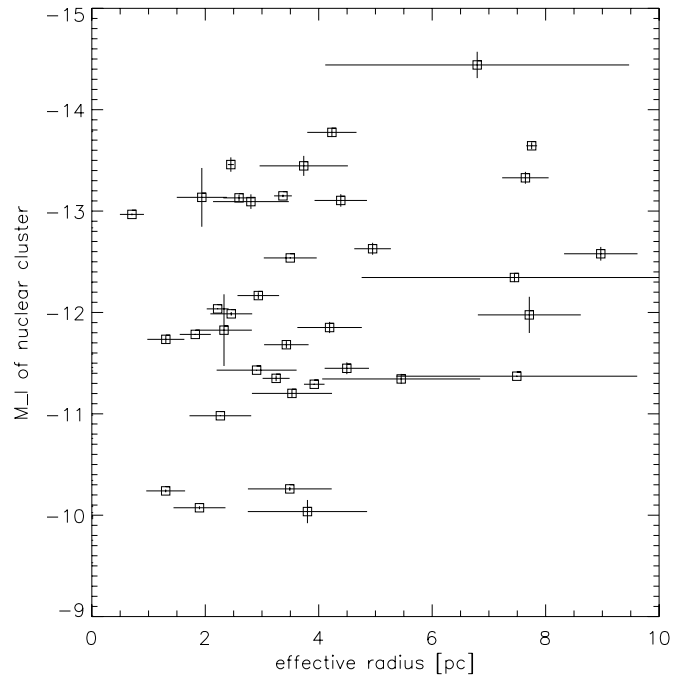

FIG. 3.—Comparison of NC effective radius and absolute magnitude. The value of r_e is not a strong function of cluster luminosity: clusters of similar size span a wide range in magnitude. Two clusters with large r_e values have been omitted from the plot in order to avoid crowding of the data points, they are the NCs in NGC 450 ($r_e = 24.3$ pc, $M_I^C = -11.96$) and NGC 4625 ($r_e = 28.8$ pc, $M_I^C = -10.63$).
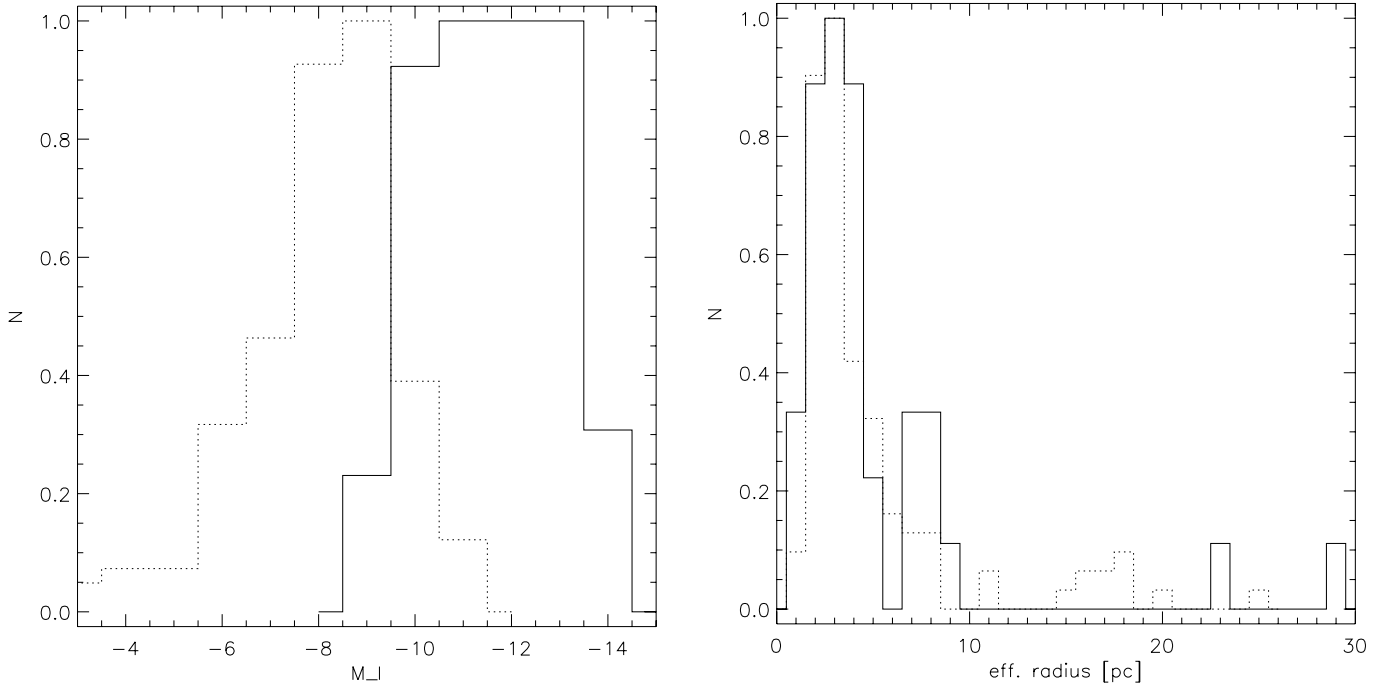
---

[8] The Milky Way GC data are taken from the February 2003 version of the online catalog compiled by Harris (1996), which contains 141 clusters with known values for angular half-light radius and heliocentric distance, King concentration index, absolute V-band magnitude, and $(B-V)$ color and excess. For 96 of these, Harris also gives an apparent $(V-I)$ color, which we correct according to $E(V-I) = 1.25E(B-V)$ (Cardelli, Clayton, & Mathis 1989) in order to derive M_I from M_V. We simply assign the average $(V-I)_0 = 0.95$ to the other 45 clusters.

FIG. 4.—*Left*: Distribution of total absolute *I*-band magnitude for all NCs of Paper I (*solid line*), compared to that of the Milky Way GCs (*dotted line*). *Right*: Distribution of effective radii for all NCs with good ISHAPE fits (*solid line*), compared to the Milky Way GCs (*dotted line*). All histograms have been normalized to a peak value of 1.
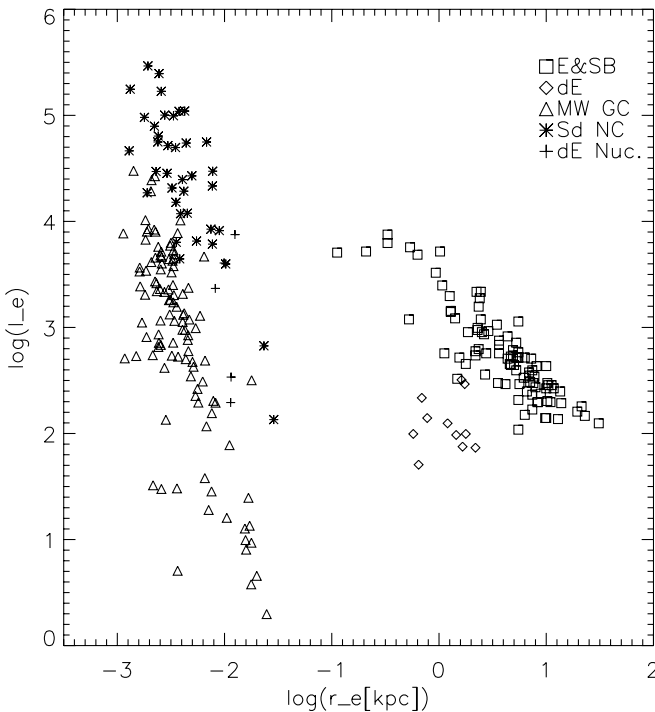

FIG. 5.—Comparison of NCs with other spheroidal populations in the r_e- vs. I_e-plane. The data are from the following sources: Galactic GCs: Harris (1996); elliptical, spiral bulge, and dE galaxies: Burstein et al. (1997); and dE nuclei: Geha et al. (2002). All photometry has been converted to the *I* band, assuming the following colors: $B-I = 2.0$ for E, S0, and dE galaxies from the Burstein et al. (1997) database, $V-I = 0.8$ for the dE nuclei of Geha et al. (2002), and $V-I = 0.95$ for those GCs that have no value for M_I listed in the Harris (1996) catalog (see § 3.1).

First, however, their identification as an extension of the GC sequence to brighter magnitudes (Fig. 4) and higher surface brightness (Fig. 5) needs to be understood in terms of *mass* rather than luminosity alone. Of particular concern in this context is the interpretation of the spread of NC absolute magnitudes in Figures 3 and 4. We consider two extreme scenarios—neither of which we mean necessarily to advocate as plausible per se, but which may serve to delimit further discussion:

1. If the stellar populations of all NCs shared a common age, then the 5 mag spread in M_I^C would translate directly to a range of a factor of ~ 100 in NC mass, intriguingly similar to the corresponding variation among old GCs (Fig. 4). Were Figure 5 then to be replotted using mass surface densities, the NC locus would simply shift vertically, by an amount depending on the typical NC age (through the *I*-band mass-to-light ratio). This would strengthen the connection of NCs to GCs and sharpen their distinction from galaxy bulges.

2. If instead all NCs had roughly the same stellar mass, then the spread in M_I^C would have to arise from a range in luminosity-weighted age, with fainter cluster magnitudes (corresponding to systematically older ages) being purely the result of stronger population fading. If this were true, then Figure 5 redrawn in terms of mass surface densities would have the NC locus contracted into a relatively narrow line of slope -2. The small variation in NC effective radius would then be largely the result of a small mass range in our sample, and it would reveal little about the (non)existence of a mass-radius relation among these clusters.

In order to gain some quantitative feel for the viability of these two alternatives, we have used the PEGASE population synthesis code (Fioc & Rocca-Volmerange 1997) to calculate the evolution of the *I*-band mass-to-light ratio and absolute magnitude for a stellar cluster of mass $7 \times 10^5 \, M_\odot$, formed in a

single burst of star formation, with the initial mass function (IMF) of Kroupa, Tout, & Gilmore (1993), between lower and upper mass cutoffs of 0.1 and 120 $M_\odot$. The results, for a range of assumed metallicities, are presented in Figure 6. Note that the mass-to-light ratio in the top panel is independent of the assumed total mass of the cluster, while the I-band magnitude in the bottom panel is of course sensitive to this parameter; for a given metallicity, the absolute magnitude of a single-burst stellar population of any mass m is obtained, as a function of age, by adding $-2.5 \log (m/7 \times 10^5 \ M_\odot)$ to the appropriate curve in Figure 6. The calculations for Υ_I and M_I^C both take into account the mass lost from a cluster as a result of stellar evolution, i.e., winds and supernova explosions.

If the NCs were, in fact, a roughly coeval population of clusters with a narrow range in mass-to-light ratio $\Upsilon_I \equiv M/L_I$ (scenario 1 above), then they could, in principle, have masses similar to the Galactic GCs if Υ_I were ~15 times smaller for NCs than for GCs (to explain the 3 mag difference in the peaks of the M_I^C distributions of Fig. 4). The top panel of Figure 6 shows that a "typical" GC, with an age of 13 Gyr and [Fe/H] = −1.5, has $\Upsilon_I \simeq 1.75 \ M_\odot \ L_\odot^{-1}$ in these models.[9] The same graph then shows that the NCs would have to be of the order of ~10^7 yr old (to within a factor of 2 or so) in order to have $\Upsilon_I \sim 0.1 \ M_\odot \ L_\odot^{-1}$, and thus a mass distribution similar to that of the GCs. Interestingly, this would make them potential

---

[9] The observed number is about 1.2 $M_\odot \ L_\odot^{-1}$, which follows from an average V-band value of 1.45 in solar units (McLaughlin 2000) and a typical $V-I$ color of 0.95 (see § 3.1).
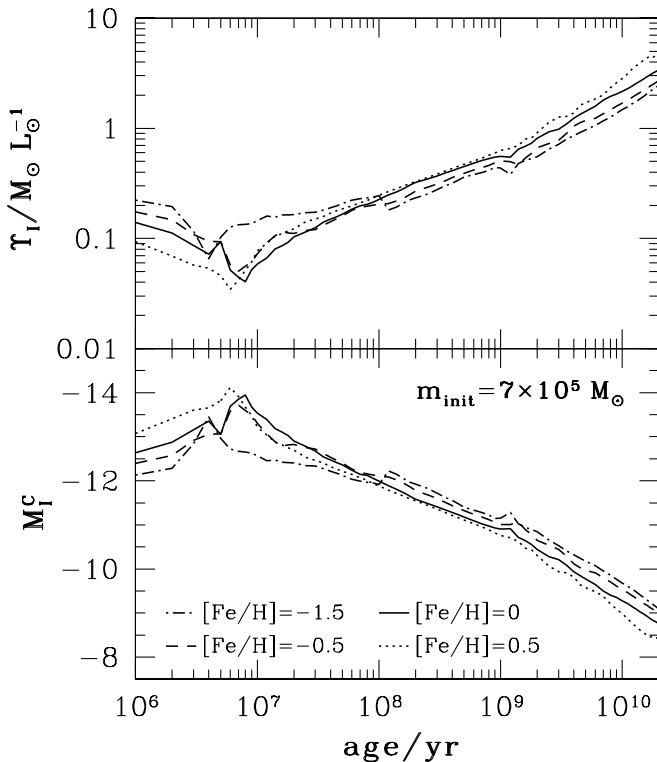

Fig. 6.—I-band mass-to-light ratio (*top*) and absolute I-band magnitude (*bottom*) for a stellar cluster of initial mass $7 \times 10^5 \ M_\odot$, formed in a single burst of star formation with the IMF of Kroupa et al. (1993) between lower and upper mass cutoffs of 0.1 and 120 $M_\odot$, as derived from the PEGASE code of Fioc & Rocca-Volmerange (1997). The predictions include the effects of mass loss due to stellar winds and supernovae, but not the effects of dynamical evolution. The four lines of each panel correspond to different metallicities, as indicated.

analogs of the super star clusters forming in many nearby interacting and starburst galaxies (see, e.g., Whitmore et al. 1999). In this context, it is worth noting that these super star clusters tend to have effective radii, $r_e \sim 2-10$ pc, that do not appear to depend strongly on luminosity, reminiscent of NCs and GCs both (see, e.g., Barth et al. 1995; Zepf et al. 1999). Nevertheless, it is difficult to imagine how such a large fraction of late-type disks could have conspired simultaneously to form NCs such a short time ago.

If, on the other hand, scenario 2 is correct and the spread in NC luminosity reflected an age spread among single-burst stellar populations with essentially a single mass, then the bottom panel of Figure 6 suggests that this common mass would have to be near $7 \times 10^5 \ M_\odot$ and the age range exceedingly broad: from 10^7 to 10^{10} yr to just barely reproduce the observed $-14 \lesssim M_I^C \lesssim -9$ (Fig. 4). (A change from the "fiducial" mass in Fig. 6 by a factor of even 2.5 in either direction would shift all the M_I^C curves up or down by a full magnitude, leaving an incomplete overlap with the observed NC magnitude distribution.)

Even as oversimplified as these two scenarios are, it is not possible to discriminate further between them without additional information. We have therefore obtained short-wavelength spectra for a number of the NCs in the current sample, which we will fit with population synthesis models to constrain the clusters' ages and star formation histories and from which we will extract stellar velocity dispersions to constrain dynamical mass-to-light ratios. Although this analysis is still in progress, the first results (Walcher et al. 2003) suggest a picture that is, not surprisingly, rather more complicated than either of the extremes just discussed.

Walcher et al. (2003) show that the light-dominating population of stars in 10 relatively bright NCs ranges in age from ~10^7 to 10^9 yr old. That is, there is in fact a spread in (luminosity-weighted) age among the NCs—although it does not appear sufficient to explain the full range of M_I^C given the single-burst models in Figure 6, unless there is *also* a significant (order-of-magnitude) spread in the cluster masses. More importantly, however, Walcher et al. (2003) show that the single-burst hypothesis itself is almost certainly incorrect; the spectra of their sample of clusters show some direct evidence for a mix of stellar ages, and the dynamical mass-to-light ratios they derive are consistently higher than the value of Υ_I inferred from population synthesis modeling, suggesting that an underlying old (faint but massive) population of stars may be present.

In view of this, and given the similarity between GC and NC effective radii, an obvious first-order enhancement over the single-burst idea is the hypothesis that NC masses are in fact dominated by old stellar populations—perhaps bona fide GCs that have been dragged by dynamical friction to the centers of their host galaxies—but that their luminosities, and hence the young ages implied by their spectra, are due mainly to more recent star formation triggered by the infall of a smaller mass of circumnuclear gas. A more thorough exploration of this scenario is beyond the scope of this paper and must await the full analysis of our spectroscopic data (Walcher et al. 2004). Nevertheless, it is worth noting that recent high-resolution interferometric studies of the nuclear gasdynamics in nearby galaxies have shown that molecular gas flows can indeed reach to within the central few parsecs of the nucleus (see, e.g., Schinnerer, Böker, & Meier 2003) and thus provide a possible mechanism for the fueling of such nuclear starburst events.

4. CORRELATIONS WITH HOST GALAXY PROPERTIES

4.1. *Luminosity and Mass of the Host Galaxy*

The work of Carollo et al. (1998) has shown that the luminosity of nuclear star clusters in early- and intermediate-type spiral galaxies correlates with the total luminosity of the host galaxy. A similar result has been established by Lotz et al. (2001) for dE galaxies. In Figure 7a, we demonstrate that such a correlation is also found in spiral galaxies at the late end of the Hubble sequence. Here we plot the apparent *I*-band magnitude of the NCs, m_I^C (from Paper I), against the total apparent blue magnitude, m_B^G, of the host galaxy (Paturel, Bottinelli, & Gouguenheim 1994), as listed in the Lyon-Meudon Extragalactic Database (LEDA).[10] The relation still holds, albeit with a somewhat larger scatter, when plotting the absolute magnitudes M_I^C and M_B^G (Fig. 7b). The conversion from apparent to absolute magnitudes and the correction for Galactic reddening was performed using the foreground extinction and galaxy distances listed in Table 1 of Paper I. The solid lines in both panels indicate the best (least-squares) linear fit to the data points. The fit coefficients, as well as their statistical significance (as measured by the Spearman rank-order coefficient), are listed in Table 2. The fact that there still is a rather good correlation with galaxy luminosity despite the large intrinsic variations of the cluster luminosities discussed in § 3.2 suggests that the global properties of the host galaxy play a significant role in the formation processes of NCs.

One possible mechanism that could link the occurrence of nuclear starbursts to the total galaxy luminosity are tidal interactions or minor mergers, because such events can both enhance the global SFR and cause significant infall of matter toward the nucleus via redistribution of angular momentum. However, as demonstrated in Figure 8, NC luminosity appears to be only weakly (if at all) correlated with the *IRAS* far-infrared (FIR) magnitude $M_{\rm FIR}$,[11] which is often used as a proxy for the SFR in galaxies (see, e.g., Telesco 1988 for a review). Assuming that tidal interactions contribute significantly to the SFR, and hence the FIR luminosity, in late-type spiral galaxies, this lack of a strong correlation between SFR and NC luminosity suggests that tidal interactions are not the driving force for the evolution of the nucleus proper. This is supported by the WFPC2 images of our galaxy sample (Paper I), which show little evidence for recent star formation activity in their (central) disks. Instead, the smooth, shallow, and undisturbed stellar disks of many late-type spiral galaxies indicate a rather uneventful dynamical history, yet most of them have a luminous NC.

An alternative explanation for the strong correlation between M_I^C and M_B^G could be that the properties of the NC are more governed by galaxy mass than by the global SFR. In principle, H I line widths could be used to address this possibility: the inclination-corrected rotational component of the H I line width,

$$W_R^i = (W_{20} - W_{\rm rand})/\sin i, \qquad (3)$$

based on the correction for random motions of Bottinelli et al. (1983), can be used as a proxy for the dynamical mass of the galaxy. Unfortunately, our galaxy sample was selected to have inclinations close to face-on, and consequently the $\sin i$

---

[10] See http://leda.univ-lyon1.fr.

[11] The apparent FIR magnitude, taken from LEDA, is calculated according to $m_{\rm FIR} = -2.5 \log (2.58 f_{60} + f_{100}) + 14.75$, where f_{60} and f_{100} are the *IRAS* fluxes at 60 and 100 μm (in janskys). This expression is identical to the one used in the RC3. The distances listed in Paper I are then used to calculate $M_{\rm FIR}$.
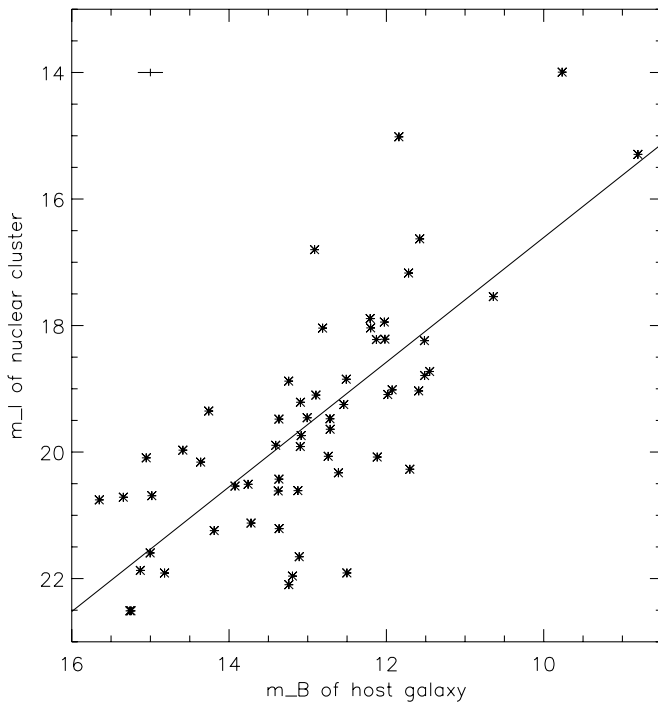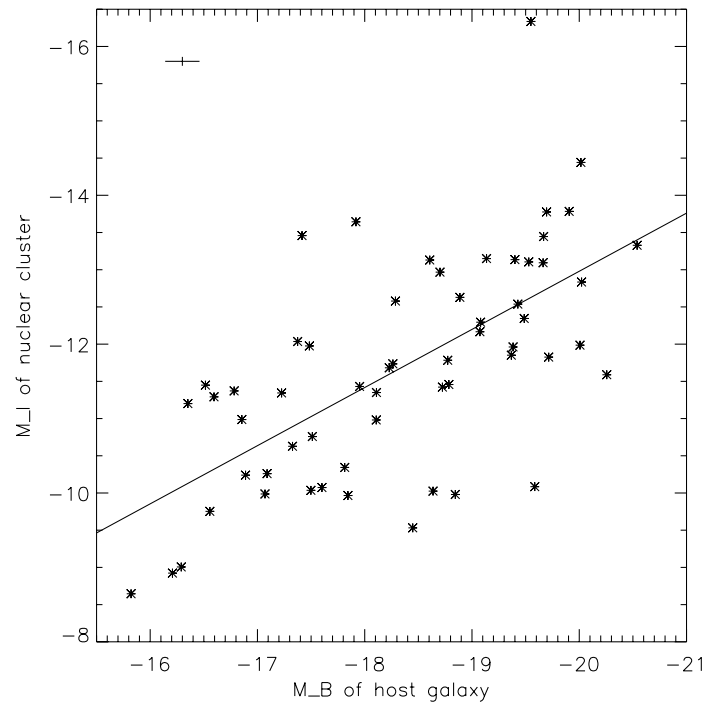

Fig. 7a

Fig. 7b

FIG. 7.—Comparison between NC luminosity and total luminosity of the host galaxy. (*a*) Apparent *I*-band magnitude of NC vs. apparent total *B*-band magnitude of the host galaxy (from the LEDA database). (*b*) Same as (*a*), but for absolute magnitudes (calculated using the distances listed in Paper I). The median error bar is indicated in the upper left-hand corner of each panel, excluding, for (*b*), any (unknown) distance errors. Both panels show a statistically significant correlation, which is indicated by the straight line in each panel. The lines mark the best least-squares linear fit to the data (fit coefficients and significance levels are given in Table 2).

TABLE 2
Fit Coefficients and Statistical Significance

x (1)	y (2)	Figure (3)	a (4)	b (5)	SROCC (6)	Significance Level (7)
m_B^G	m_I^C	7a	6.8 ± 1.5	0.99 ± 0.11	0.757	5.762
M_B^G	M_I^C	7b	2.6 ± 2.3	0.78 ± 0.13	0.654	4.978
M_{FIR}^G	M_I^C	8	-2.0 ± 3.7	0.53 ± 0.20	0.420	2.554
μ_I^0	M_B^G	9a	-29.2 ± 1.6	0.60 ± 0.09	0.679	5.173
μ_I^0	M_I^C	9b	-25.2 ± 0.6	0.75 ± 0.11	0.627	4.778

Notes.—Cols. (1–3): Quantities to be correlated using the expression $y = a + b \times x$ and figure in which they are plotted against each other. Cols. (4) and (5): Coefficients a and b of best linear least-squares fit, together with their statistical uncertainties (1 σ). Cols. (6) and (7): Spearman rank-order correlation coefficient (SROCC) and significance (standard deviations) of correlation.

corrections are highly uncertain. For the sake of completeness, we have nevertheless calculated the galaxy masses with the above expression. Following Matthews, van Driel, & Gallagher (1998), we adopted $W_{rand} = 20$ km s^{-1} for our galaxies, which corresponds to a line-of-sight velocity dispersion $\sigma_z = 5.5$ km s^{-1} (Rhee 1996). However, using the inclination i as listed in LEDA, we found that for our sample, the H I width does not even correlate with total galaxy luminosity, which is a contradiction of the Tully-Fisher relation. We thus conclude that for our sample of face-on spiral galaxies, W_R^i is not a reliable indicator of galaxy mass and that we therefore cannot draw any meaningful conclusions about possible correlations of NC properties and host galaxy mass.

4.2. Central Surface Brightness of the Galaxy Disk

Recent analysis of large galaxy samples (see, e.g., Blanton et al. 2003) has put on a solid statistical ground the notion that there are strong correlations between a number of physical properties of galaxies. In particular, Blanton et al. (2003) have shown that for disk-dominated, "exponential" galaxies (i.e.,
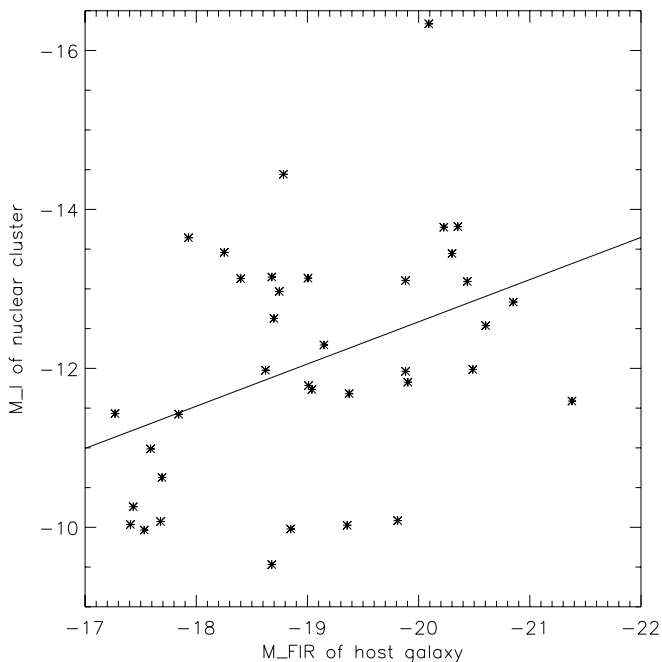

Fig. 8.—I-band magnitude of NC vs. IRAS FIR magnitude of the host galaxy (from the LEDA database). Over the luminosity range of our galaxy sample, only a weak correlation exists. The lines mark the best least-squares linear fit to the data. The fit coefficients and significance levels are given in Table 2.

with Sérsic 1968 shape parameter $n < 1.5$), surface brightness correlates with total luminosity. We confirm this finding for our sample, as demonstrated in Figure 9a. Here we have plotted M_B^G, the total blue magnitude of the host galaxy, versus μ_I^0, the central I-band surface brightness of the stellar disk underlying the NC. The values for μ_I^0 are listed in column (3) of Table 1; they were measured from our WFPC2 images by averaging the two inward extrapolations of the surface brightness profile shown in Figure 3 of Paper I at a radius of $0\farcs024$ (i.e., the border of the central WFPC2 pixel).

Given that NC luminosity M_I^C correlates with host galaxy luminosity (Fig. 7b) and that the latter correlates with μ_I^0, it is not surprising that M_I^C is also correlated with μ_I^0, as demonstrated in Figure 9b. Again, the fit coefficients and significance levels of both correlations are listed in Table 2. While it is true in general that higher surface brightness disks make it more difficult to detect faint clusters, we emphasize that this effect does not result in a significant selection bias. In fact, most galaxies without a clear identification of an NC have μ_I^0 values *below average* (Fig. 4 of Paper I). Note that the values of μ_I^0 are as observed; i.e., they have not been corrected for inclination.

So far, we have shown that more luminous galaxies have higher surface brightness disks, as well as more luminous NCs. Is this simply a reflection of the popular notion that "bigger galaxies have more of everything"? While this is certainly part of the answer, it is likely not the whole story. This is demonstrated in Figure 10, which plots M_I^C as well as the cluster-to-disk luminosity ratio C/D as functions of the physical size of the galaxy disk, i.e., the major axis diameter of the $\mu_B = 25$ isophote as listed in LEDA. (The disk luminosity is calculated as total galaxy luminosity minus NC luminosity, but with $C/D \lesssim 0.01$ in general the disk light is not significantly different from the total galaxy luminosity.)

Apparently, M_I^C depends weakly on galaxy size: the Spearman rank-order correlation coefficient in Figure 10a is $s = 0.36$, with slightly less than 3 σ significance. However, this actually reflects the stronger and more significant correlation between NC luminosity and galaxy luminosity (§ 4.1), coupled with a similarly significant dependence of disk size on total disk luminosity: $R_{disk} \sim L_{disk}^{0.32}$ in this sample. From Table 2 we see that NC luminosity scales with galaxy (disk) luminosity as $L_{cl} \sim L_{disk}^{0.78}$, and thus we can expect $C/D \equiv (L_{cl}/L_{disk}) \sim L_{disk}^{-0.22} \sim R_{disk}^{-0.69}$, even if there is no *direct* connection between NC luminosity and global disk size. This scaling is indeed consistent with the weak trend in Figure 10b.

To first order, the NC luminosity is a measure of the efficiency with which gas is funneled toward the nucleus and converted into stars, regardless of the exact star formation history of the NC. This is true even if the cluster luminosity
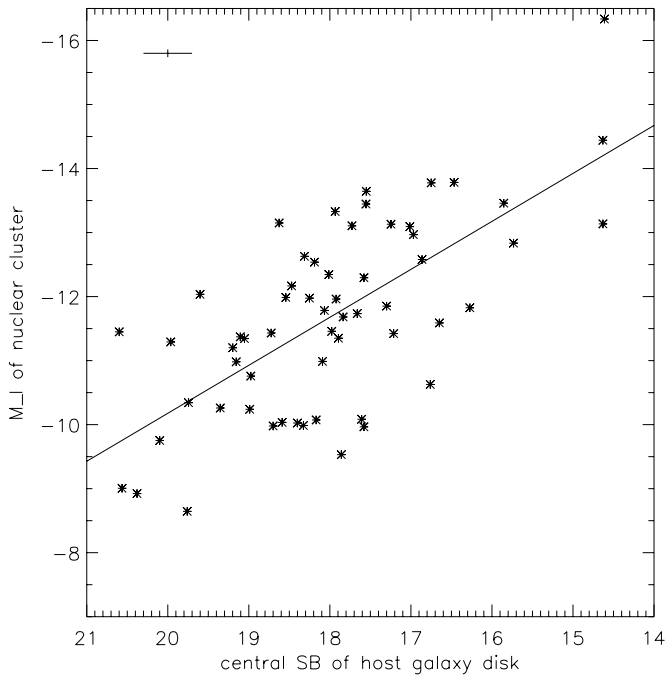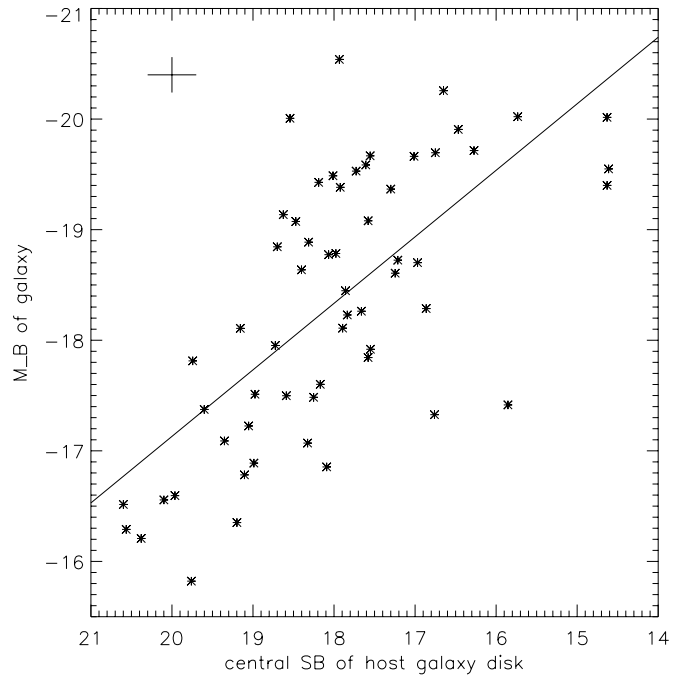
Fig. 9a

Fig. 9b

FIG. 9.—(a) *I*-band magnitude of nuclear star cluster, M_I^C, and (b) total blue galaxy magnitude M_B^G, as a function of central disk surface brightness μ_I^0. All three quantities are correlated with each other.

is dominated by a minor (in mass) but recent burst, because on average, younger populations imply a higher duty cycle of nuclear "delta" bursts. It thus appears that, at least to some degree, the mechanisms that regulate the (past) star formation efficiency in the vicinity of the galaxy nucleus, as traced by the central surface brightness of its stellar disk, also play a significant role in determining the amount of gas that is funneled

into the central few parsecs and converted into stars. Further support for this notion comes from the fact that the molecular gas content within the central kiloparsec of late-type spiral galaxies also appears to be connected to the disk surface brightness in the sense that low surface brightness disks in general have little or no central molecular gas (Fig. 7 of Böker, Lisenfeld, & Schinnerer 2003a).
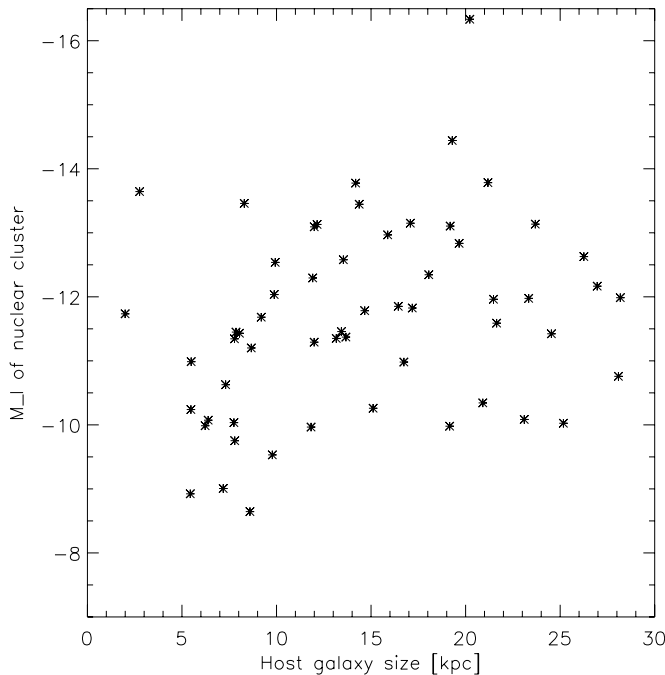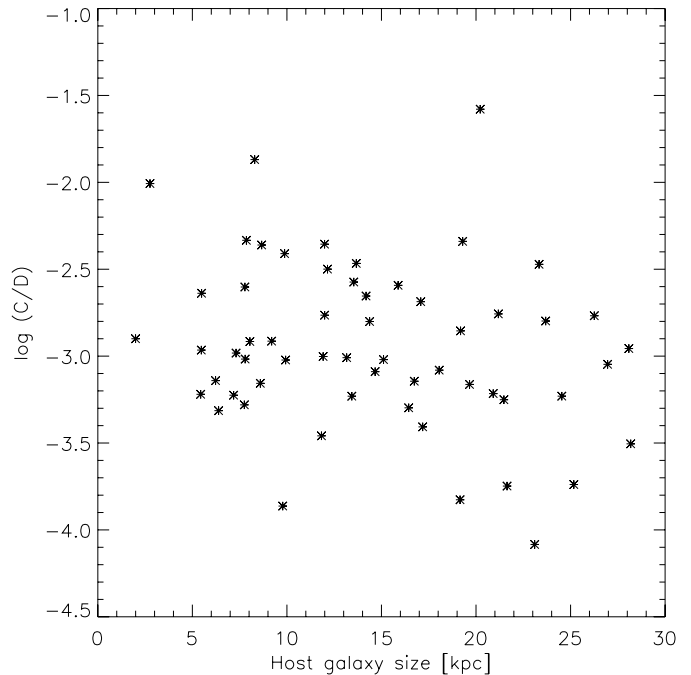

Fig. 10a

Fig. 10b

FIG. 10.—(a) *I*-band magnitude of nuclear star cluster, M_I^C, and (b) cluster-to-disk luminosity ratio *C/D* as a function of physical isophotal diameter of the galaxy disk. Any apparent trend can be explained by the strong correlation between cluster luminosity and galaxy luminosity (see text).
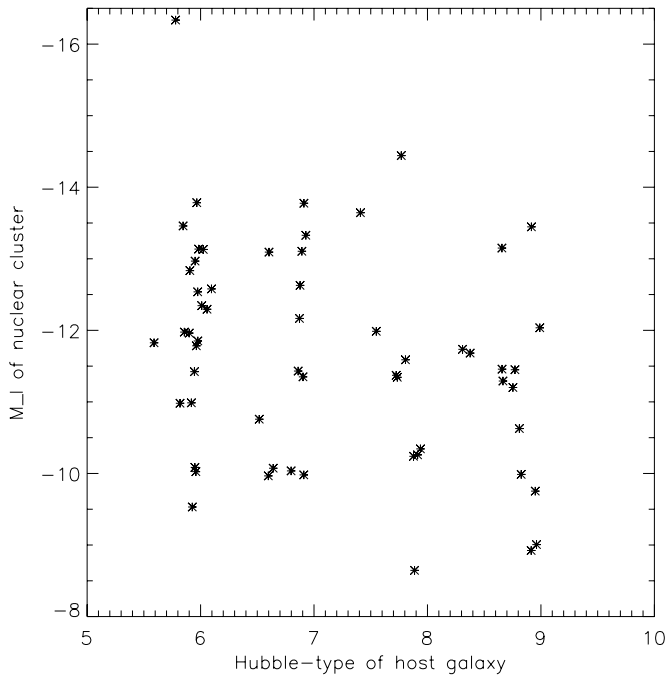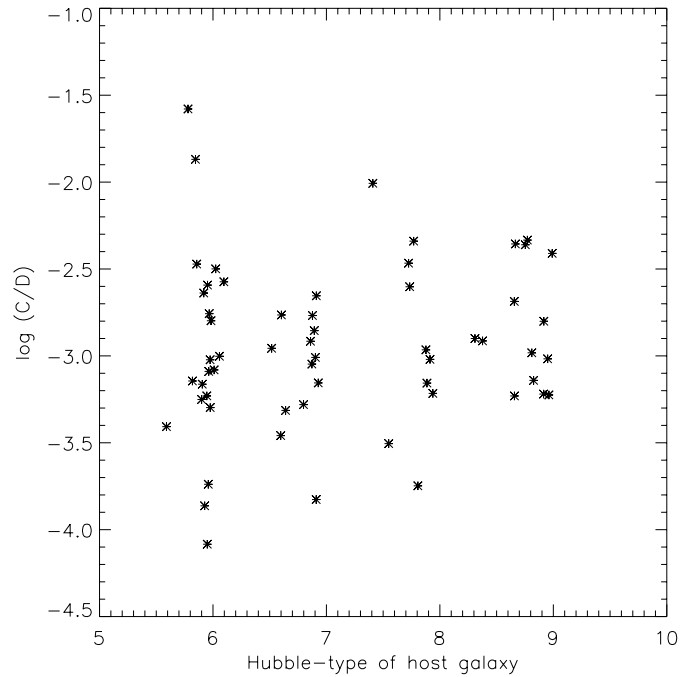
Fig. 11a

Fig. 11b

Fig. 11.—(a) I-band magnitude of nuclear star cluster, M_I^C, and (b) cluster-to-disk luminosity ratio C/D as a function of galaxy Hubble type. No trends are apparent.

4.3. Hubble Type

Figure 11a compares NC absolute magnitudes against the Hubble type of their host galaxies. The very weak correlation apparent here, with a Spearman coefficient $s = -0.26$, is only marginally significant (at the 2 σ level, and less if the cluster in NGC 7418, with $M_I^C = -16.33$, is excluded). It seems in any case to be the result of the strong link between NC and total galaxy luminosities, together with a trend toward slightly fainter galaxy magnitudes, on average, for the later Hubble types. Figure 11b therefore plots the ratio of cluster-to-disk luminosity versus Hubble type. The correlation coefficient in this case is only $s = 0.13$, which is not significant at even the 1 σ level.

Thus, NC luminosity is essentially independent of Hubble type. This should not come as a surprise given that the Hubble type is not a strong discriminant for the latest type spiral galaxies, as discussed in more detail by Böker, Stanek, & van der Marel (2003b). The main reason is that the NC is quite easily mistaken for a compact stellar bulge in seeing-limited images, and hence a ground-based morphological classification based at least in part on the bulge-to-disk ratio is inaccurate at best.

4.4. Nuclear Clusters and Stellar Bars

Using the morphological classifications of our galaxy sample, from both the RC3 (listed in Table 1 of Paper I) and the LEDA database, we have investigated for our complete Paper I sample whether nuclear star clusters are more likely to be found in (or whether they preferentially avoid) galaxies of a certain bar class. Table 3 summarizes the statistics for both subsamples with (59 galaxies) and without (18 galaxies) an NC. The fraction of galaxies with an NC is 76%, 88%, and 67% for the RC3 classifications A, AB, and B, respectively. The LEDA database only lists the types "unbarred" and "barred"; for these, the corresponding fractions are 88% and 73%. The apparently smaller frequency of NCs in barred galaxies is probably not significant, given the small number statistics in

some categories and the rather high number of uncertain classifications (17 galaxies in our sample are classified as either uncertain or peculiar in the RC3). More reliable classifications of the morphology of late-type spiral galaxies will require a more accurate isophotal analysis or even kinematic information on their central disks.

This rough analysis suggests that the galaxy bar class is not a significant factor for the likelihood of hosting an NC. In particular, the late-type galaxies in our sample seem to have no special difficulty in supporting bars and NCs simultaneously. This might seem somewhat paradoxical in the light of some early numerical simulations of barred galaxies, which found that fairly modest central mass concentrations could drive dynamical instabilities that destroyed the bar on rather short timescales (see, e.g., Friedli 1994; Norman et al. 1996).

TABLE 3

IMPACT OF BAR CLASS ON NUCLEAR CLUSTER FREQUENCY

Class	With NC	Without NC
RC3		
Unbarred (A)...........	76% (16)	24% (5)
Mixed (AB).............	88% (23)	12% (3)
Barred (B)...............	67% (20)	33% (10)
Total	77% (59)	23% (18)
LEDA		
Unbarred.................	88% (15)	12% (2)
Barred.....................	73% (44)	27% (16)
Total	77% (59)	23% (18)

NOTES.—Sample fraction and total number of galaxies with and without a clearly identified NC, sorted by bar classification. For comparison, we have listed the statistics for both the RC3 and LEDA databases.

However, more recent work (Shen & Sellwood 2003[12]) suggests that even an NC as massive as a few percent of the total disk mass of a galaxy (i.e., with $C/D \gtrsim 0.02$, already much higher than the typical values in Fig. 10b) may not be able to destroy a bar completely within a Hubble time. It is then somewhat unclear what role bars and NCs together might play in the formation of the exponential "pseudobulges" found in many late-type spiral galaxies (cf. Carollo et al. 2001).

5. SUMMARY

We have presented a structural analysis of 39 nuclear star clusters in late-type spiral galaxies. After correction for the instrumental PSF, we measure a median effective radius for the sample of $\bar{r}_e = 3.5$ pc, with 50% of the sample falling in the range 2.4 pc $\leq r_e \leq$ 5.0 pc. This narrow size distribution is statistically indistinguishable from that of Galactic GCs, even though the NCs are on average 4 mag brighter than the old GCs. The compactness of NCs clearly separates them from larger ellipsoidal stellar systems, such as spiral bulges or elliptical galaxies.

In addition, we have compared the luminosity of NCs with various properties of their host galaxies. We find that NC luminosity correlates with galaxy luminosity, which extends a previous result obtained for earlier-type spiral galaxies. Because there is a strong correlation between total luminosity and central disk surface brightness for the galaxies in our sample, NC luminosity also correlates with local disk brightness. It is

not clear which of these trends is physically more fundamental. Either way, other apparent correlations, such as between cluster luminosity and galaxy size, can ultimately be explained by the underlying link to galaxy luminosity and/or central disk surface brightness.

We find no systematic trends with the Hubble type of the galaxy, confirming that the latter is not a strong discriminant for the latest type spiral galaxies. We also find no evidence for a connection between the presence/absence of NCs and the presence/absence of large-scale stellar bars in the host galaxy.

Without additional spectral information, it is not possible to put strong constraints on the formation history of NCs. We suggest that the most likely scenario for NC formation consists of multiple nuclear starbursts, possibly caused by gas infall onto a "seed" cluster. However, a more detailed discussion of this hypothesis has to await the analysis of our spectroscopic data, which we will present in a future paper.

---

[12] Shen & Sellwood (2003) is available at http://www.ociw.edu/ociw/symposia/series/symposium1/proceedings.html.

REFERENCES

Barmby, P., Holland, S., & Huchra, J. P. 2002, AJ, 123, 1937
Barth, A. J., Ho, L. C., Filippenko, A. V., & Sargent, W. L. 1995, AJ, 110, 1009
Bender, R., Burstein, D., & Faber, S. M. 1992, ApJ, 399, 462
Blanton, M. R., et al. 2003, ApJ, 594, 186
Böker, T., Laine, S., van der Marel, R. P., Sarzi, M., Rix, H.-W., Ho, L., & Shields, J. C. 2002, AJ, 123, 1389 (Paper I)
Böker, T., Lisenfeld, U., & Schinnerer, E. 2003a, A&A, 406, 87
Böker, T., Stanek, R., & van der Marel, R. P. 2003b, AJ, 125, 1073
Böker, T., van der Marel, R. P., Mazzuca, L., Rix, H.-W., Rudnick, G., Ho, L., & Shields, J. C. 2001, AJ, 121, 1473
Böker, T., van der Marel, R. P., & Vacca, W. D. 1999, AJ, 118, 831
Bottinelli, L., Goughenheim, L., Paturel, G., & de Vaucouleurs, G. 1983, A&A, 118, 4
Burch, S. F., Gull, S. F., & Skilling, J. 1983, Comput. Vision Graph. Image Proc., 23, 113
Burstein, D., Bender, R., Faber, S., & Nolthenius, R. 1997, AJ, 114, 1365
Cardelli, J. A., Clayton, G. C., & Mathis, J. S. 1989, ApJ, 345, 245
Carlberg, R. G. 1992, ApJ, 399, L31
Carlson, M. N., & Holtzman, J. A. 2001, PASP, 113, 1522
Carollo, C. M. 1999, ApJ, 523, 566
Carollo, C. M., Stiavelli, M., de Zeeuw, P. T., Seigar, M., & Dejonghe, H. 2001, ApJ, 546, 216
Carollo, C. M., Stiavelli, M., & Mack, J. 1998, AJ, 116, 68
Davidge, T. J., & Courteau, S. 2002, AJ, 123, 1438
Djorgovski, S., & Meylan, G. 1994, AJ, 108, 1292
Ferrarese, L., & Merritt, D. 2000, ApJ, 539, L9
Fioc, M., & Rocca-Volmerange, B. 1997, A&A, 326, 950
Friedli, D. 1994, in Mass-Transfer Induced Activity in Galaxies, ed. I. Shlosman (Cambridge: Cambridge Univ. Press), 268
Gebhardt, K., et al. 2000, ApJ, 539, L13
Geha, M., Guhathakurta, P., & van der Marel, R. P. 2002, AJ, 124, 3073
Gordon, K. D., Hanson, M. M., Clayton, G. C., Rieke, G. H., & Misselt, K. A. 1999, ApJ, 519, 165
Harris, W. E. 1996, AJ, 112, 1487
Harris, W. E., Harris, G. L. H., Holland, S. T., & McLaughlin, D. E. 2002, AJ, 124, 1435
Holtzman, J. A., et al. 1992, AJ, 103, 691

King, I. R. 1962, AJ, 67, 471
Kormendy, J. 1985, ApJ, 295, 73
Krist, J., & Hook, R. 2001, The TinyTim User's Guide, version 6.0 (Baltimore: STScI)
Kroupa, P., Tout, C. A., & Gilmore, G. 1993, MNRAS, 262, 545
Kundu, A., & Whitmore, B. C. 1998, AJ, 116, 2841
Larsen, S. S. 1999, A&AS, 139, 393
———. 2002, AJ, 124, 1393
Larsen, S. S., Brodie, J. P., Sarajedini, A., & Huchra, J. P. 2002a, AJ, 124, 2615
Larsen, S. S., Efremov, Y. N., Elmegreen, B. G., Alfaro, E. J., Battinelli, P., Hodge, P. W., & Richtler, T. 2002b, ApJ, 567, 896
Lotz, J., Telford, R., Ferguson, H. C., Miller, B. W., Stiavelli, M., & Mack, J. 2001, ApJ, 552, 572
Lucy, L. B. 1974, AJ, 79, 745
Maoz, D., Barth, A. J., Ho, L. C., Sternberg, A., & Filippenko, A. V. 2001, AJ, 121, 3048
Matthews, L. D., & Gallagher, J. S., III 1997, AJ, 114, 1899
Matthews, L. D., van Driel, W., & Gallagher, J. S., III 1998, AJ, 116, 2196
Matthews, L. D., et al. 1999, AJ, 118, 208
McLaughlin, D. E. 2000, ApJ, 539, 618
Mengel, S., Lehnert, M. D., Thatte, N., & Genzel, R. 2002, A&A, 383, 137
Norman, C. A., Sellwood, J. A., & Hasan, H. 1996, ApJ, 462, 114
Paturel, G., Bottinelli, L., & Gouguenheim, L. 1994, A&A, 286, 768
Phillips, A. C., Illingworth, G. D., MacKenty, J. W., & Franx, M. 1996, AJ, 111, 1566
Press, W. H., Teukolsky, S. A., Vetterling, W. T., & Flannery, B. P. 1992, Numerical Recipes in C. The Art of Scientific Computing (Cambridge: Cambridge Univ. Press)
Rhee, M.-H. 1996, Ph.D. thesis, Univ. Groningen
Richardson, W. H. 1972, J. Opt. Soc. Am., 62, 55
Schinnerer, E., Böker, T., & Meier, D. S. 2003, ApJ, 591, L115
Sérsic, J.-L. 1968, Atlas de Galaxias Australes (Cordoba: Obs. Astron.)
Shen, J., & Sellwood, J. A. 2003, Carnegie Observatories Astrophysics Series, Vol. 1: Coevolution of Black Holes and Galaxies, ed. L. C. Ho (Pasadena: Carnegie Observatories)
Smith, L. J., & Gallagher, J. S., III 2001, MNRAS, 326, 1027
Telesco, C. M. 1988, ARA&A, 26, 343

van den Bergh, S., Morbey, C., & Pazder, J. 1991, ApJ, 375, 594
Walcher, C. J., et al. 2003, Carnegie Observatories Astrophysics Series, Vol. 1:
    Coevolution of Black Holes and Galaxies, ed. L. C. Ho (Pasadena: Carnegie
    Observatories)
———. 2004, in preparation

Whitmore, B. C., Zhang, Q., Leitherer, C., Fall, S. M., Schweizer, F., & Miller,
    B. W. 1999, AJ, 118, 1551
Zepf, S. E., Ashman, K. M., English, J., Freeman, K. C., & Sharples, R. M.
    1999, AJ, 118, 752